Improved surface carrier recombination and efficiency for selective emitter N-type solar cells with Al-alloyed rear junction

CHENG-YI HSU[a], BING-LUN CAI[b], CHIEN-HUNG WU[b,*], YULI LIN[a]
[a]College of Engineering, Chung Hua University, Hsinchu, Taiwan, R.O.C
[b]Department of Electronics Engineering, Chung Hua University, Hsinchu, Taiwan, R.O.C

In this paper, a fabrication process using well-arranged $n^+n/n^{++}n$ front surface fields (FSFs) and a low temperature phosphosilicate glass (LTPSG) oxidation/etching for the emitter of n-type crystalline silicon solar cells is demonstrated. With an optimized phosphorus diffusion temperature of around 835°C and a 6-min LTPSG oxidation, an effective lifetime for minority charge carriers, as long as 285.94 μs and a high efficiency of 19.2% under AM 1.5 were obtained. This improved cell performance is attributed to the enhanced collection efficiency of excitons from FSFs and a good surface passivation from the oxidation/etching process to reduce surface recombination velocity.

1. Introduction

For the past decades, n-type silicon wafers have been widely used for high-efficiency solar cells due to their electrically superior properties compared to p-type Si, such as higher tolerance of metal impurities, better stability under illumination, and higher minority carrier lifetime [1-6]. Many publications have presented cells made with front contacts and a full Al-alloyed p^+ junction on the rear formed by a firing process of screen-printed Al paste. Furthermore, a cost-effective method to fabricate n-type solar cells has been demonstrated by using the combination of Al-alloyed emitter and a phosphorous doped FSF [7-9]. Screen printed Al paste, followed by post firing process, onto the rear side of n-type silicon substrate can simply form p^+ layer, instead of typical high-temperature boron diffusion by tube furnace [10-13]. Applying the standard processing sequence to n-type silicon leads to a rear emitter solar cell with a phosphorous FSF [14]. Without the constraints of heavy doping for maintaining good ohmic contact, emitter profiles can be optimized to achieve lower emitter saturation current densities (J_{0e}). As a result, such emitters should yield higher V_{OC} values in completed solar cells. It is well known that lower J_{0e} values can be achieved for phosphorus emitters by lowering the surface concentration.

Since most of the charge carriers are generated close to the front surface but are collected at the rear emitter, a high bulk lifetime and low front surface recombination velocity (SRV) are crucial for achieving high efficiencies with this solar cell type [8-15]. Large area n-type silicon solar cells with a screen-printed Al-alloyed rear junction are mainly limited by their front surface recombination velocity. In order to overcome this limitation, a simple and industrially applicable production sequence that use a LTPSG oxidation etch back and create a selective front surface field (s-FSF) for n-type silicon solar cells is proposed in this work. The improvements in suppressing SRV and increasing emitter lifetime were applied step by step to demonstrate the advantages of the proposed solar cells. The experimental characteristics of all the prepared samples, such as J_{0e}, V_{OC}, J_{SC}, fill factor (F.F.), external quantum efficiency (EQE), conversion efficiency (η), etc. are presented and discussed.

2. Experimental procedure

First, n-type Czochralski (CZ) Si (100) substrates of 200 μm thicknesses and a resistivity of 1–2 Ω-cm were cleaned by standard RCA-1 cleaning processes. Second, the pyramidal structures were formed by a wet chemical etching using a solution of KOH, isopropyl alcohol (IPA), and deionized (DI) water at a temperature of 80°C for 30 min. Front phosphorus emitters with different sheet resistances were diffused from a POCl3 source at different temperatures.

Considering cells with conventional rear junction structure are usually limited by Auger recombination on the FSF, n^+/n and n^{++}/n high low junctions were employed for the cell emitter through phosphorus diffusion. Note that the former creates a homogenous front surface field (h-FSF), while the latter builds a selective front surface

field (s-FSF) [16-19] under the cathode electrode. In addition, we used LTPSG oxidation and then etch back via a short dilute-HF dip to passivate surface region of the lightly-doped n$^+$ emitter. An antireflective layer of SiNx film with a thickness of about 90 nm was deposited on the front side of the silicon substrate by plasma enhanced chemical vapor deposition (PECVD). After that, Ag paste and Al paste were used as the front contact and rear contact, respectively. Note that the finger space and width of the front contact were 2 mm and 100 nm, respectively. The peak temperature for co-firing was 770°C. Finally, the samples were then isolated using a laser.

3. Results and discussion

In n-type crystalline Si, the Shockley–Read–Hall recombination is relatively unimportant. In contrast, the Auger recombination can be significant especially under high level injection conditions. Likewise, the emitter surface recombination velocity of minority carrier should also play an important part in determining the collection efficiency of photo excited carriers. The emitter saturation current density J_{0e} can be evaluated by the following equation [20],

$$\frac{1}{\tau_{eff}} \approx \frac{1}{\tau_{bulk}} + \frac{1}{\tau_{Aug}} + \frac{2J_{0e}(\Delta n + N_{dop})}{qWn_i^2} \qquad (1)$$

Where τ_{eff}, τ_{bulk}, and τ_{Aug} are the effective life time, bulk life time, and auger life time, respectively. Δn, W, n_i, and N_{dop} are the excess electron density, the total width of the sample, intrinsic carrier concentration in silicon, and doping concentration of the cell. Note that the plot of $1/\tau_{eff}$ -$1/\tau_{Aug}$ vs. Δn would show a constant slope that is attributable to recombination in the diffused regions.

The dark current of p-n-junction cells can be described by the 2-diode model [21]. Since J_{0e} is the major part of the emitter saturation current, the open-circuit voltage V_{OC} is strongly affected by J_{0e} through the well-known relationship of $V_{oc} \approx (nkT/q)\ln(J_{sc}/J_{0e})$ [22-23]. It is of very crucial to maximize the emitter life time to realize a J_{0e} as small as possible to improve the cell performance. In our work, a selective-emitter cell which has a low contact resistance due to heavy doping underneath the screen-printing metal grid, an improved front-surface passivation of the lightly doped region between the grid, and the use of h-FSF and s-FSF to reduced recombination under the metal contact have been fabricated by oxidation etching back process successfully.

Fig. 1 shows the measured external quantum efficiency (EQE) of the prepared cells as a function of wavelength λ for all splits of the diffusion temperature. The SIMS data inserted in Fig. 1 illustrates the doping profiles of the samples under different P diffusion temperatures. It is evident that the diffusion temperature

of 835°C yields the highest EQE, especially, in the short wavelength region 300-500 nm. It could be due to a lightly doped emitter providing a good surface passivation which could not only increase short-wavelength absorption, but also suppress the diffusion current in emitter region. As a result, the minority carrier lifetime, open-circuit voltage, and conversion efficiency could be improved.
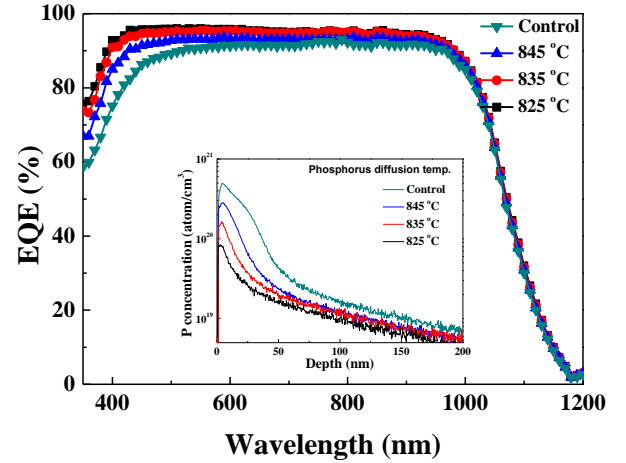
Fig. 1. SIMS and EQE data for phosphorus concentration profiles annealed at different temperatures, control sample, 825°C, 835°C, and 845°C

Fig. 2(a) shows the $1/\tau_{eff}$ -$1/\tau_{Aug}$ vs. ΔN relationship for samples with phosphorus doped at different temperatures. It reveals that the 835°C-P-doped sample has a relatively lower J_{0e} of around 330 fA/cm^2 and effective lifetime of 140.08 μs. Referring to the control sample with J_{0e} of 690 fA/cm^2 and effective lifetime of 52.23 μs, such a result indicates that carrier recombination in this region could have been effectively suppressed. To further optimize the phosphorus concentration of the emitter, the PSG growth time was examined and results were shown in Fig. 2(b) for the 835°C-P-doped cases with the PSG growth times as a parameter. It is seen that the highest effective lifetime of 180.3 μs with the lowest J_{0e} of 270 fA/cm^2 emitter can be realized for the cases with the PSG growth time of 6 min, indicating carrier recombination near surface regions have been further suppressed. With the emitter doping concentration obtained at 835°C for 6 min, LTPSG oxidation was followed to passivate surface region of the lightly-doped emitter. As a result, the improved J_{0e} of 32 fA/cm^2 and effective lifetime of 285.94 μs can be realized as shown in Fig. 2(c).

(a)

(b)

(c)
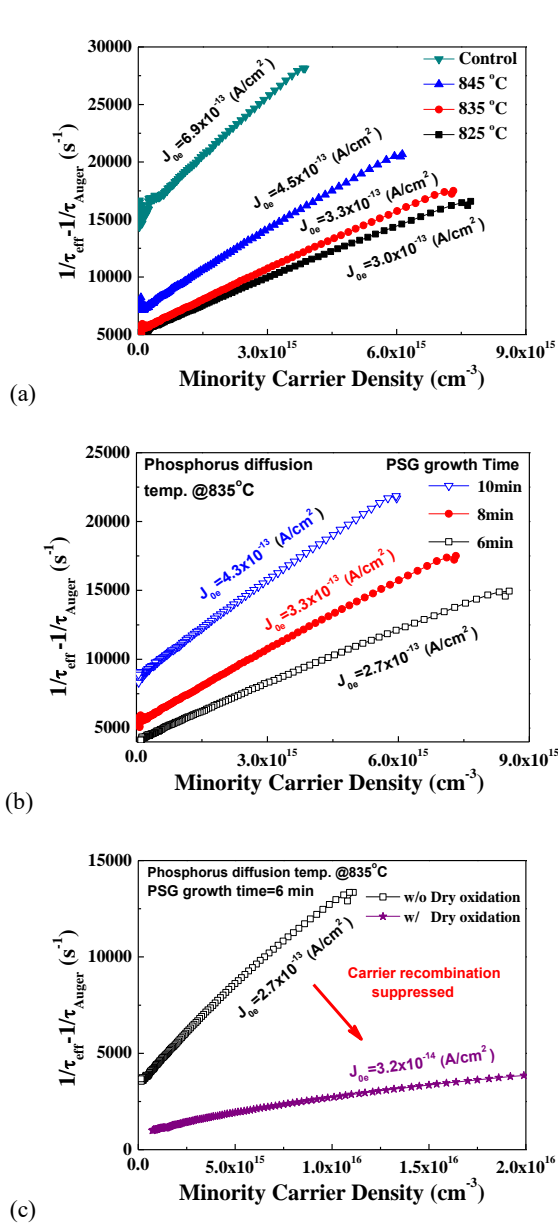
Fig. 2. Measured inverse lifetime as a function of the minority carrier density. (a) phosphorus concentration profiles annealed at different temperatures, control sample, 825ºC, 835ºC, and 845ºC. (b) PSG growth time at 835 ºC is 6 min, 8 min, and 10 min. (c) surface treatment with or without LTPSG oxidation

Fig. 3 shows the measured I-V characteristics of the prepared solar cell based on the proposed emitter doping and LTPSG oxidation processes. Under AM 1.5G, high short-circuit current of about 37.05 mA/cm^2, open-circuit voltage of about 0.644 V, good fill factor of about 80.4% and effective conversion efficiency of about 19.2% were achieved, which is mainly attributed to the considerable reduction in the dark current of the proposed emitter. Table 1 summarizes the cell electrical parameters under AM1.5G with different surface conditions for the n-Si solar cells.
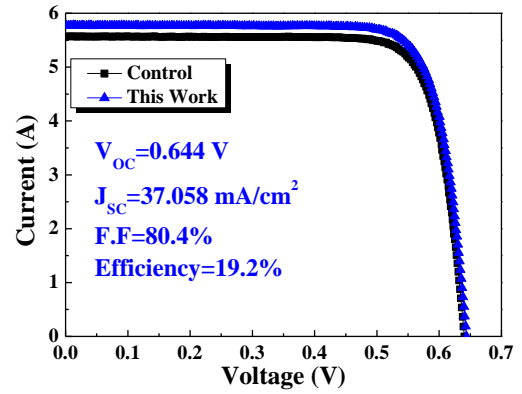
Fig. 3. I-V characteristics of the 19.2% n-type solar cell (AM1.5G)

Table 1.

Process condition	J_{0e} [fA/cm^2]	Jsc [mA/cm^2]	Voc [V]	F.F. [%]	Cell eff. [%]
control	690	34.539	0.625	79.7	17.211
P diffusion temp. 845℃	450	35.088	0.632	79.9	17.792
P diffusion temp. 835℃	330	35.556	0.635	79.9	18.020
P diffusion temp. 825℃	300	35.640	0.634	79.5	17.946
This work at 835℃ (optimize)	32	37.058	0.644	80.4	19.202

4. Conclusion

An n-Si solar cell with improved performance via front surface passivation using lightly-doped emitter structure and surface passivation using LTPSG oxidation etch back process have been presented. Our work has demonstrated that the surface recombination of minority carriers can be effectively suppressed with a light-doped emitter of 835ºC for 6 min process. It has also shown that the LTPSG oxidation layers, passivated on the front side, not only improved the effective lifetime but also enhanced front internal carrier transport. As a result, both J_{SC} and V_{OC} could be improved and a certified cell efficiency for the n-type solar cells at 19.2%, V_{OC} at 0.644V, J_{SC} at 37.05 mA/cm^2 and FF at 80.4%, respectively.

References

[1] K. Ryu, A. Upadhyaya, Y. W. Ok, M. H. Kang, V. Upadhyaya, L. Metin, H. Xu, A. Bhanap, A. Rohatgi, IEEE Electron Devices **33**(12), 584 (2012).

[2] A. Cuevas, M. J. Kerr, C. Samundsett, Appl. Phys. Lett. **81**(26), 4952 (2002).

[3] D. Macdonald, L. J. Geerligs, Appl. Phys. Lett. **85**(18), 4061 (2004).

[4] J. E. Cotter, J. H. Guo, P. J. Cousins, M. D. Abbott, F. W. Chen, K. C. Fisher, IEEE Trans. Electron Devices **53**(8), 1893 (2006).

[5] Y. Komatsu, V. D. Mihailetchi, L. J. Geerligs, B. van Dijk, J. B. Rem, M. Harris, Solar Energy Mater. Solar Cells **93**(6-7), 750 (2009).

[6] R. Bock, J. Schmidt, R. Brendel, Appl. Phys. Lett. **91**(11), 112112 (2007).

[7] C. Schmiga, H. Nagel, J. Schmidt, Prog. Photovolt. Res. Appl. **14**(6), 533 (2006).

[8] C. Schmiga, M. Hermle, S. W. Glunz, in Proc. 23rd Eur. Photovolt. Solar Energy Conf. pp. 982 (2008).

[9] R. Bock, J. Schmidt, R. Brendel, Phys. Stat. Sol. **2**(6), 248 (2008).

[10] M. Rüdiger, C. Schmiga, M. Rauer, M. Hermle, S. W. Glunz, IEEE Transactions Electron Devices **59**(5), 1295 (2012).

[11] A. Sugianto, M. Ly, M. B. Edwards, B. S. Tjahjono, S. R. Wenham, IEEE Transactions Electron Devices **57**(2), 525 (2010).

[12] F. Book, T. Wiedenmann, S. Gloger, B. Raabe, G. Schubert, H. Plagwitz, G. Hahn, in 26th European Photovoltaic Solar Energy Conference pp. 1160 (2011).

[13] C. Schmiga, M. Rauer, M. Rüdiger, K. Meyer, J. Lossen, H.-J. Krokoszinski, M. Hermle, S. W. Glunz, in 25th European Photovoltaic Solar Energy Conference pp. 1163 (2010).

[14] D. L. Meier, H. P. Davis, R. A. Garcia, J. Salami, A. Rohatgi, A. Ebong, P. Doshi, Solar Energy Materials & Solar Cells **65**(1-4), 621 (2001).

[15] F. Book, T. Wiedenmann, G. Schubert, H. Plagwitz, G. Hahn, Energy Procedia **8**, 487 (2011). S. P. Su, N. Chantarat, Y. H. Huang, C. M. Kang, S. H. T. Chen, L. W. Cheng, in 38th IEEE pp. 001010 (2012).

[16] F. Book, T. Wiedenmann, A. Dastgheib-Shirazi, B. Raabe, G. Hahn, in 25th European Photovoltaic Solar energy Conference and Exhibition/ 5th World Conference on Photovoltaic Energy Conversion pp. 1465(2010).

[17] M. Rudiger, C. Schmiga, M. Rauer, M. Hermle, S. W. Glunz, in 25th European Photovoltaic Solar energy Conference and Exhibition/ 5th World Conference on Photovoltaic Energy Conversion pp. 2280 (2010).

[18] R. Bock, R. Hesse, J. Schmidt, R. Brendel, J. Maier, B. Geyer, J. Koopmann, H. Kerp, in 25th European Photovoltaic Solar energy Conference and Exhibition/ 5th World Conference on Photovoltaic Energy Conversion pp. 1449 (2010).

[19] A. Cuevas, Sol. En. Mat. Sol. Cells **57**(3), 277 (1999).

[20] O. Breitenstein, Solar Energy Materials & Solar Cells **95**(10), 2933 (2011).

[21] U. J̈ager, S. Mack, C. Wufka, A. Wolf, D. Biro, R. Preu, IEEE Journal of Photovoltaics **3**(2), 621 (2013).

[22] S. Mack, C. Wufka, A. Wolf, U. Belledin, D. Scheffler, D. Biro, Energy Procedia **8**, 343 (2011).

*Corresponding author: rossiwu@chu.edu.tw